Luminosity and Performance of DØ during the First Year of Run 2

Sung Hwan Ahn,[3] Oleksiy Atramentov,[2] Michael Begel,[7] Gregor Geurkov,[1] John Hauptman,[2] Alexander Kupčo,[6] Seh Wook Lee,[3] Prolay Kumar Mal,[8] Chyi-Chang Miao,[1] Jae Won Park,[3] Richard Partridge,[1] Heidi Schellman,[5] Marco Verzocchi[4]

[1] *Brown University, Providence, Rhode Island*
[2] *State University, Ames, Iowa*
[3] *Korea University, Seoul, Korea*
[4] *University of Maryland, College Park, Maryland*
[5] *Northwestern University, Evanston, Illinois*
[6] *Center for Particle Physics, Prague, Czech Republic*
[7] *University of Rochester, Rochester, New York*
[8] *Tata Institute of Fundamental Research, Mumbia, India*

August 30, 2002

The role of the Luminosity ID group is to measure, record, and provide normalization information for DØ physics analyses, provide feedback on beam conditions to DØ Operations and Beams Division, and report on luminosity and operations to the DØ leadership and the Fermilab Directorate. The group maintains an independent data acquisition system that collates real-time information from all major online systems, stores the data for later retrieval, and displays the data in the DØ control room. This report describes our operations during the first year of Run 2A.

1 Introduction

Run 2 began with an engineering period July through November 2000. Most of the CDF detector was in the B0 collision hall; DØ elected not to roll in the detector. The Luminosity group placed a set of Run 1 Level 0 counters [1] on a stand in the DØ collision hall. The beam was used to commission the Run 1 FastZ electronics [1, 2] that we continued to use throughout

the beginning of Run 2. The Forward Proton group also instrumented several Roman pot detectors; the luminosity detector was used to form a diffractive trigger. DØ received its initial luminosity at $\sqrt{s} = 1.96$ TeV on October 8, 2000 and accumulated ≈ 80 nb^{-1} during the engineering period.

The official start of Run 2 was March 1, 2001. Luminosity was first delivered on April 3, 2001. The early stores consisted of one proton bunch colliding with eight anti-proton bunches (1×8, one collision each at B0 and D0) and were used primarily for timing studies. The first 36×36 store occurred on April 27, 2001. Initial luminosities were $< 1 \times 10^{30}\ cm^{-2}s^{-1}$ for these early stores. The record peak luminosity of $2.48 \times 10^{31}\ cm^{-2}s^{-1}$ occurred on July 26, 2002 (the goal for Run 2A is $20 \times 10^{31}\ cm^{-2}s^{-1}$). The accelerator complex started up very slowly in Run 2; a comparison of the luminosity delivered to DØ as a function of colliding days (excluding all shutdowns at least one day in length) for Runs 1A, 1B, and 2A is shown in Fig. 1.

The first physics run of Run 2A was recorded on August 24, 2001. This report covers the period from October 8, 2000 through August 23, 2002.

2 Luminosity Monitor

The Luminosity Monitor (LM) was designed to measure the luminosity of collisions at the DØ interaction region [3]. The LM consists of plastic scintillaters read-out via photomultipliers. There are 24 wedges mounted on the inside edge of each end-cap calorimeter cryostat at $z \approx \pm 140\ cm$ (Fig. 2). These wedges are arrayed around the beam pipe as shown in Fig. 3. The detector covers $2.7 < |\eta| < 4.4$. The overall acceptance of the Run 2 detector is similar to that of the Run 1 L0 detector (Fig. 4). Each wedge consists of 5/8 *in* thick BC-408 scintillator with 1 *in* diameter fine-mesh Hamamatsu R5505 photomultiplier tubes mounted directly on the face. The counters are located in a region where the solenoid produces a nearly axial magnetic field of ≈ 1 Tesla. The photomultiplier tubes have a relative gain of $> 10\,000$ at 1 Tesla. The LM was designed to have time-of-flight resolution of $\approx 200\ ps$ [4].

The LM uses the time difference between signals produced by the north and south detectors to differentiate between collisions (luminosity) and beam losses (halo). We are currently using the Run 1 NIM-based FastZ modules to perform this identification [1, 2]. Signals from wedges in each half of the detector are summed together and used as inputs to the FastZ. The FastZ compares the time difference between the summed north and summed south signals to independently identify luminosity and halo.

Protons travel clockwise around the Tevatron, so a muon produced by an errant proton (i.e., proton halo) will first pass through the north LM, and then, $\approx 9\ ns$ later, pass through the south LM. Anti-protons travel counter-clockwise around the Tevatron, so anti-proton halo will first hit the south LM and then the north LM. This is illustrated in Figs. 5 and 6. On the other hand, particles produced in collisions between protons and anti-protons in the DØ interaction region should strike the north and south LM at approximately the same time (Fig. 7). The difference between north and south is used to determine the Z of the interaction.

Two pictures of the output of a QVT module are shown in Fig. 2. Time increases from right to left so the earliest signal is associated with the north LM — the proton halo. The

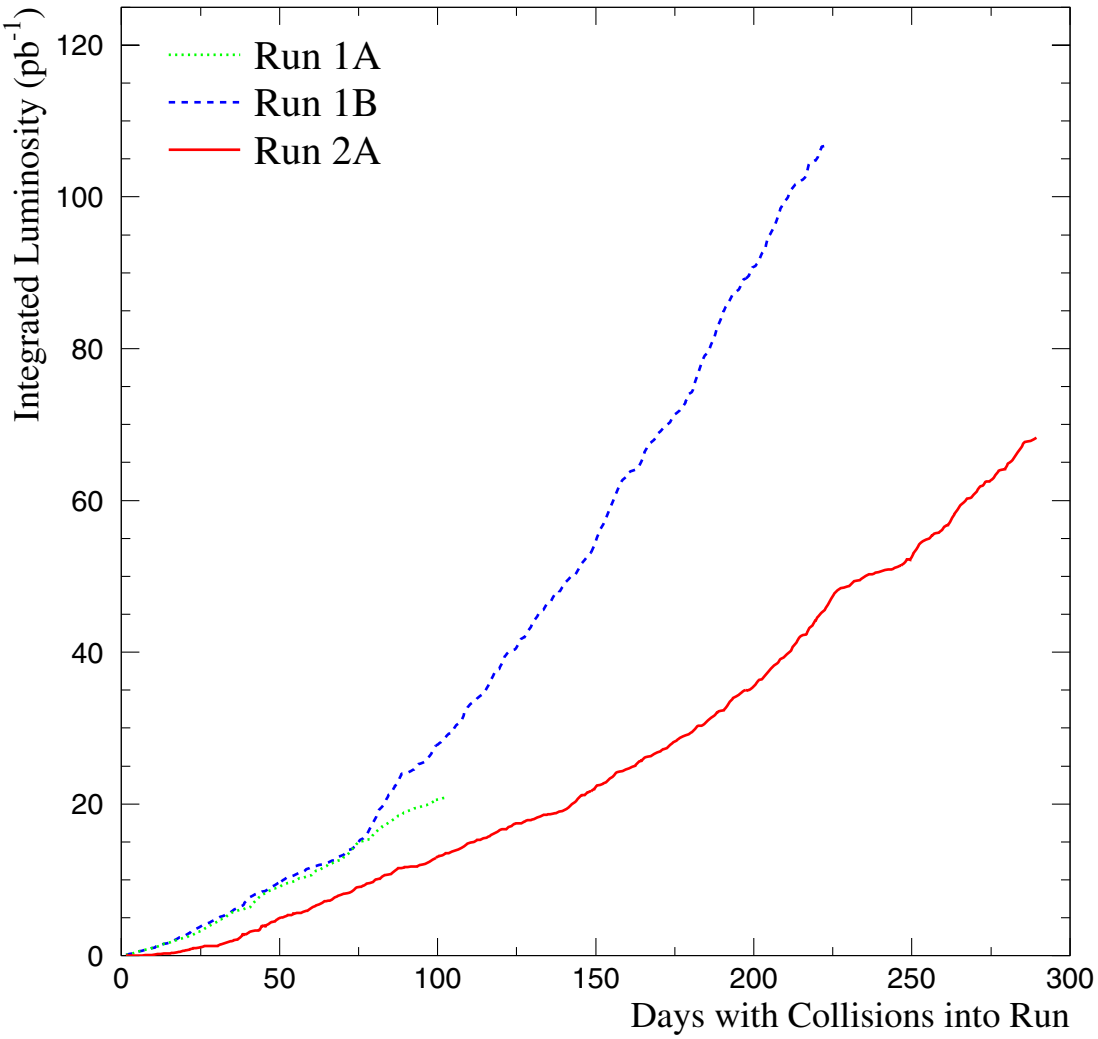

Figure 1: Luminosity delivered to DØ during Runs 1A (dotted), 1B (dashed), and 2A (solid) as a function of days with collisions into the Run. This exludes all shutdowns of at least one day in length. First collisions for Run 2A occurred on April 3, 2001.

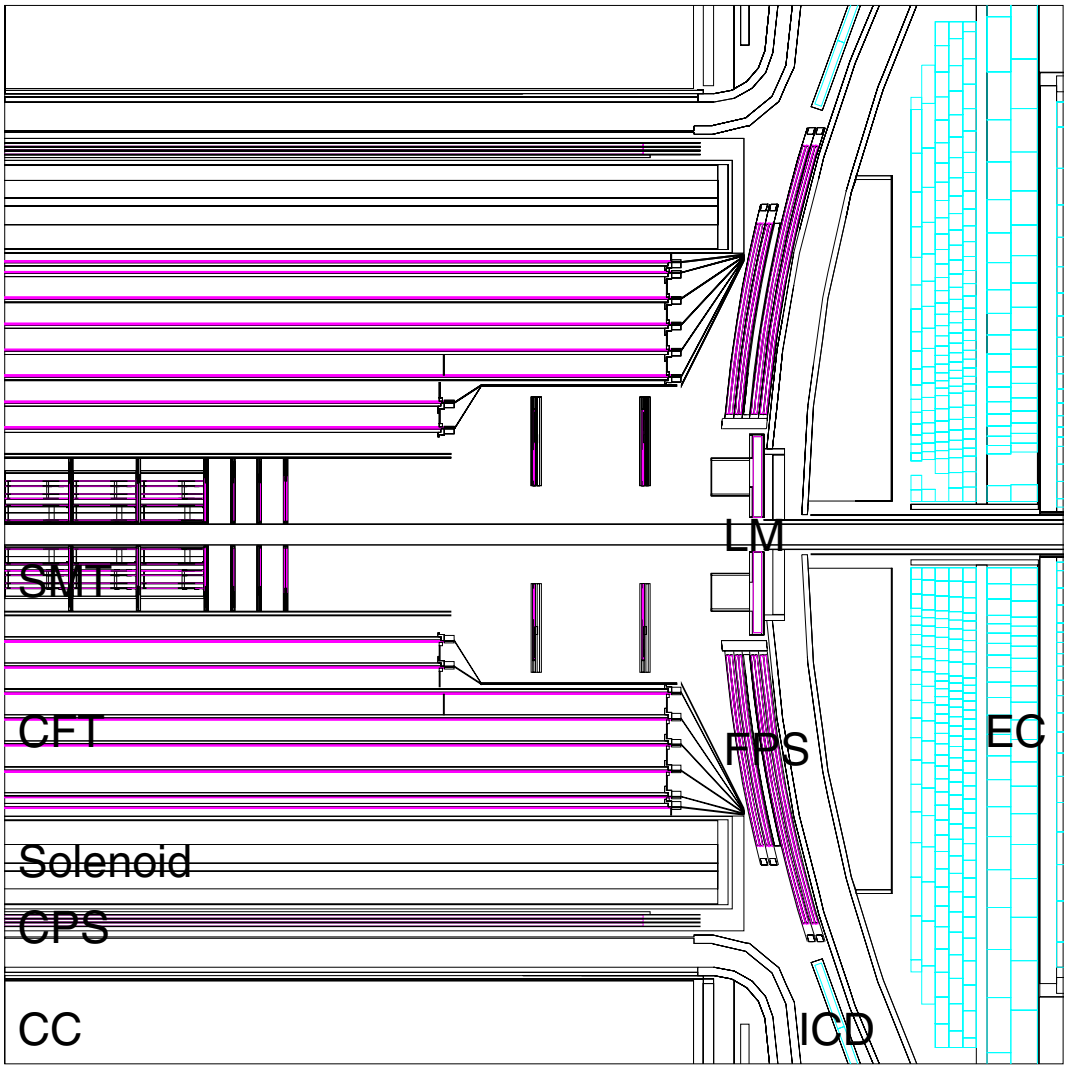

Figure 2: Cut-view of the DØ detector focussing on the Luminosity Monitor (LM).

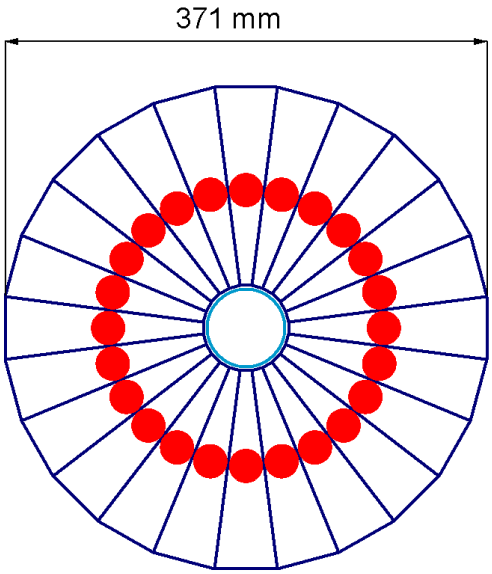

Figure 3: Schematic of the Run 2 Luminosity Monitor (one side). The solid circles represent the locations of the photomultiplier tubes.

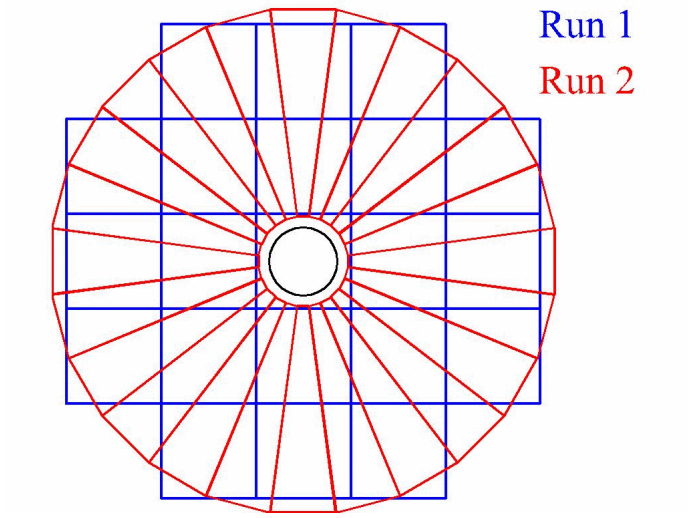

Figure 4: Schematic overlay of the Run 1 (squares) and Run 2 (wedges) luminosity detectors.

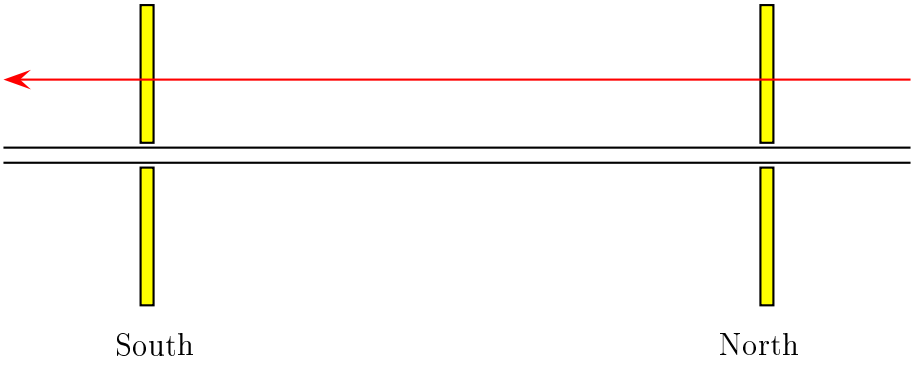

Figure 5: Cartoon showing how proton halo interacts in time with the Luminosity Monitor.

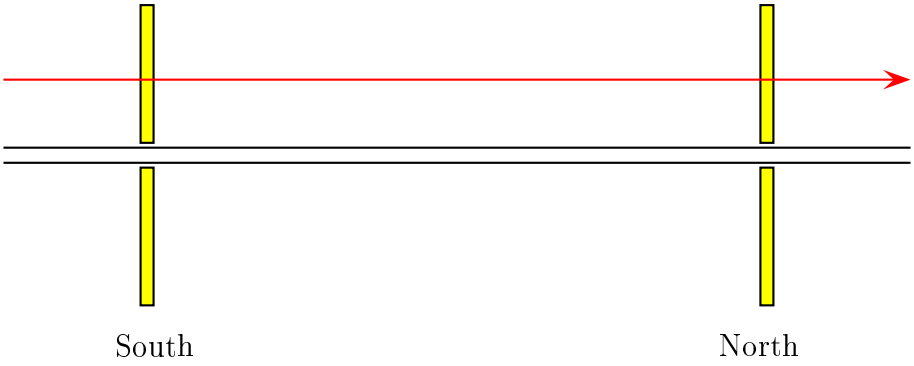

Figure 6: Cartoon showing how anti-proton halo interact in time with the Luminosity Monitor.

central peak (around $t = 0$) represents collisions (the area under the peak is proportional to the luminosity), and the left-most peak is due to anti-proton halo. The picture on the left was taken in October 2000 — the first luminosity signal observed during the Run 2 engineering period. The other picture (right) was taken one year later. The improvement in the luminosity delivered to DØ is easily apparent.

The FastZ modules use a set of gates to distinguish between collisions and halo. The time difference between the north and south hits is also used to measure the Z-position of the interaction; the FastZ modules have a resolution of $\approx 6.25\ cm$ in Z. All of these signals: luminosity, proton halo, anti-proton halo, and the Z-position of the interaction (digitized in five bits), are sent to the Trigger Framework as And/Or terms for use in Level 1 trigger decisions [5].

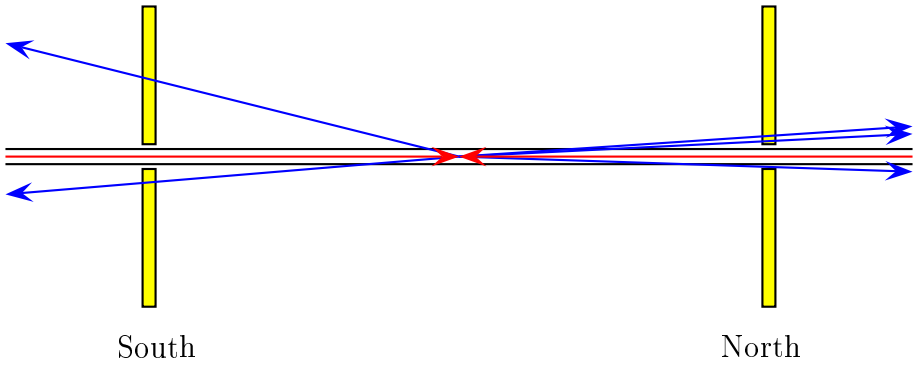

Figure 7: Cartoon showing the luminosity time signature in the Luminosity Monitor.

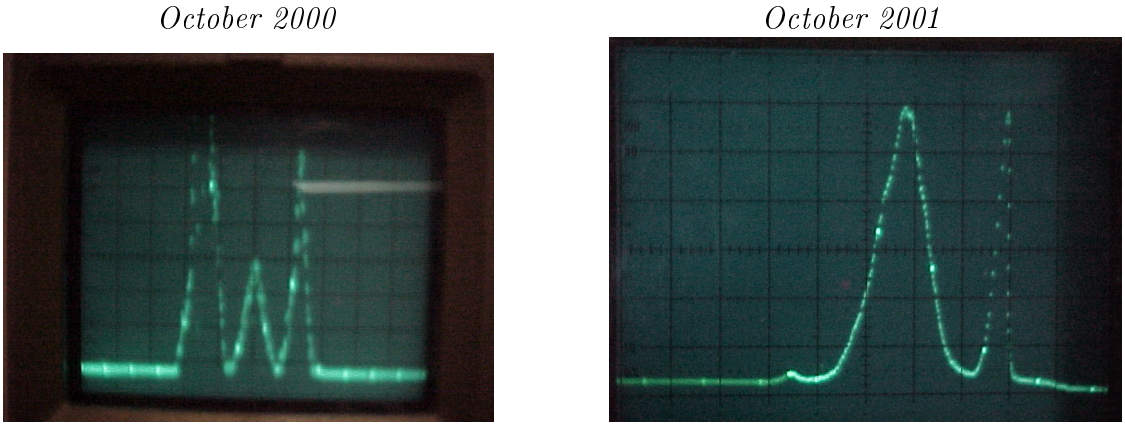

Figure 8: Oscilloscope screen shots of the output from a QVT module; the picture on the left was taken in October 2000, the picture on the right was taken in October 2001. Within each picture, the right-most peak (earliest in time) is due to proton halo, the left-most peak (latest in time) is due to anti-proton halo, and the central peak is luminosity.

3 Luminosity Data Acquisition

The Luminosity data acquisition system ($\mathcal{L}$DAQ) is a stand-alone DAQ running on the Online cluster [6]. The $\mathcal{L}$DAQ was designed to collect sufficient data to measure, verify, and monitor the luminosity delivered to and used by DØ. The framework was modelled as a distributed client/server based on the intertask communications protocol (ITC) used by other parts of the Online system [7, 8, 9]. Applications are written in Python [10] with classes that inherit from a wrapped ITC processor class. The schematic for the present system is displayed in Fig. 3. Each $\mathcal{L}$DAQ application connects to command & control applications and to a monitoring process [11].

The $\mathcal{L}$DAQ connects to the following systems: L1 Trigger Framework via the Trigger Control Computer [12], Accelerator Controls System (ACNET) [13], DØ Controls System (EPICS) [14], Level 3 (both DAQ [15] and ScriptRunner [16]), COOR [17] (via the brun and erun files), and Datalogger (via the event catalogs). Data for every LBN is archived to disk. These LBN files are validated once per day; data from different sources are correlated and loaded into a private data base (Python shelf). This is used for producing reports, offline normalization files [18], and as inputs to external analysis tools.

4 Luminosity Block

The luminosity block is the fundamental unit of time for the luminosity measurement. Each block is indexed by the luminosity block number (LBN), which monotonically increases throughout Run 2. The LBN is incremented upon run or store transitions, TFW or SCL inits, by request, or after 60 seconds have elapsed. The time span was chosen based on numerous constraints in the luminosity, trigger, and DAQ systems. The time period is short enough so that the instantaneous luminosity is effectively constant during each luminosity block, introducing negligible uncertainty into the measurement of the luminosity due to the width of the time slice. Raw data files (partitions) are opened and closed on LBN boundaries. Luminosity calculations are made independently for each LBN. Results are averaged over the luminosity block.

5 Luminosity Calculation

The luminosity calculation is detailed in DØ Notes 3970, 3971, and 3972 [19, 20, 21]. The delivered luminosity is based on the output from the FastZ electronics. These outputs are counted by VME scalers located within the TFW. The delivered luminosity is defined by

$$\mathcal{L} = -\frac{f/159}{\sigma} \sum_{i=1}^{159} \ln\left(1 - \frac{\Delta LM_i}{\Delta ticks/159}\right), \tag{1}$$

where f is the Tevatron revolution frequency, σ is the effective $p\bar{p}$ cross section for satisfying the LM coincidence, ΔLM_i is the scaler count from the LM for tick i, and $\Delta ticks$ is the length of the luminosity block in 132 ns ticks. Note that the delivered luminosity is calculated independently for each of the 159 ticks and summed.

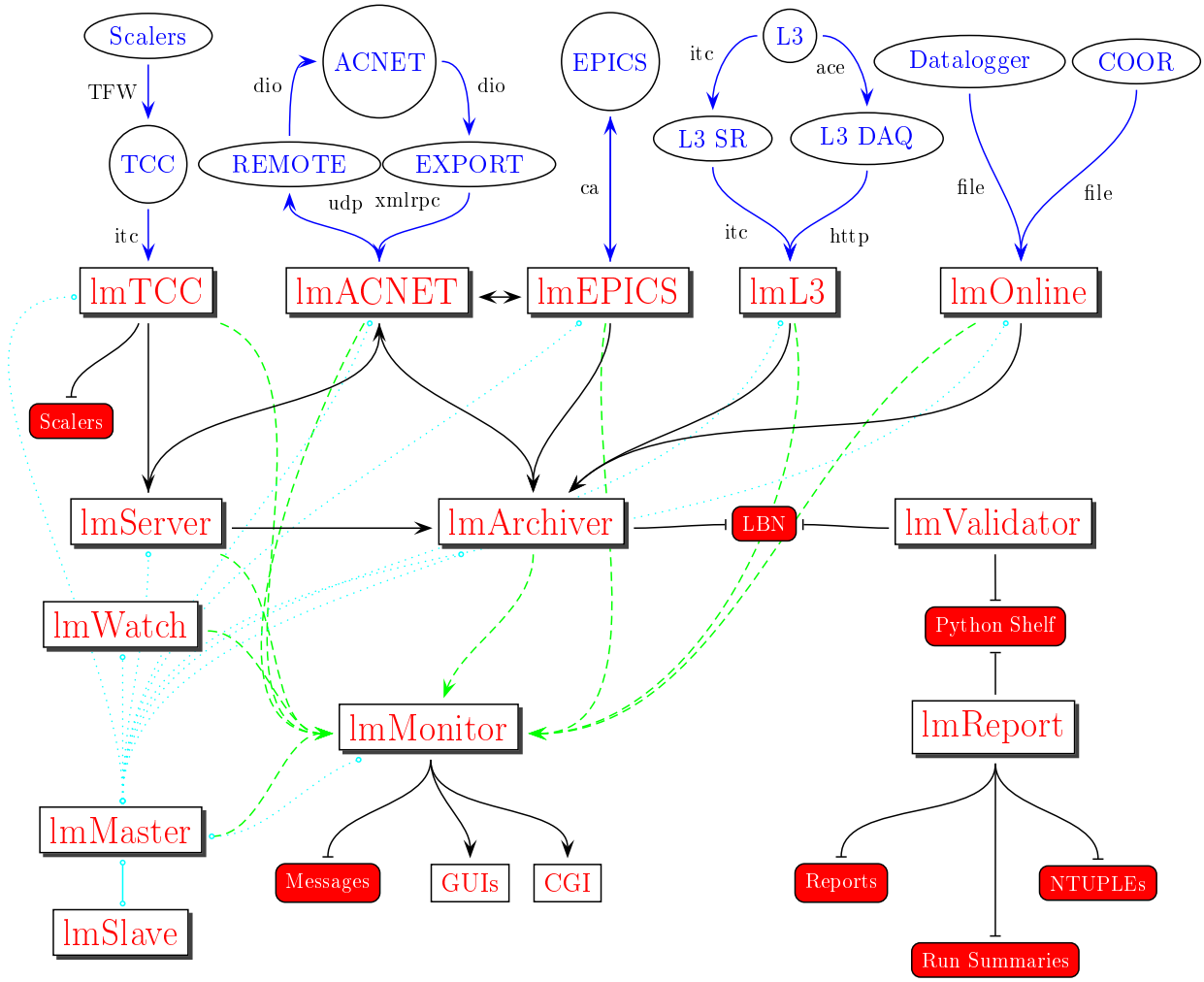

Figure 9: Schema of the luminosity data acquisition system showing all connections between applications. $\mathcal{L}$DAQ applications are represented by shadowed boxes, $\mathcal{L}$DAQ files are filled rounded rectangles, and outside applications are circles and ovals. Solid lines represent data paths between applications, dashed lines indicate monitoring paths, while dotted lines indicate command & control paths.

The proper determination of the Luminosity constant, σ, has historically been a contentious issue at DØ, and between DØ, CDF, and Beams Division. For the data sample in this report, we use 43 mb. This value was adopted at the end of Run 1B [22]. While the efficiency and acceptance of the Run 2 LM are different than the Level 0 detector from Run 1, and while the $\sqrt{s}$ is larger and the world average of some of the underlying cross sections have changed, we believe that these effects are probably small ($< 10\%$). The uncertainty of the luminosity discussed in this report is order 10%.

The luminosity for L1 triggers is described in DØ Note 3971 [20]. Triggers are grouped together so that they have common dead-time, i.e., common sources of enable, disable, and readout. These groups are called Exposure Groups [12, 23, 24]. The exposure group definition includes all And/Or terms (AOT) [5] that are highly correlated with the bunch structure (e.g., the live-beam-crossing term). Other such terms include any AOT that causes a bias in the normalization such as requiring a single interaction, a tight Z cut on the primary vertex, or a veto on an LM output (exposure groups containing these AOT terms cannot be normalized according to the methodology described in this report). Exposure groups allow the readout to be partitioned so that different triggers may read-out independent portions of the detector.

A L1 trigger is defined by a set of AOT (including all terms required by its exposure group) and belongs to one, and only one, exposure group. The calculation for the L1 trigger luminosity follows from Eq. 1,

$$\mathcal{L}_{L1}(n) = \frac{\Delta decorrelated_n}{\Delta ticks} \sum_{i=1}^{159} \frac{\Delta correlated_i}{\Delta ticks/159} \mathcal{L}_i. \tag{2}$$

where $\mathcal{L}_i$ is the delivered luminosity in tick i. $\Delta correlated$ includes the effects of all AOT and disables correlated with the bunch-to-bunch luminosity profile (hence the separate accounting for the 159 ticks) including some global disables (e.g. skip next crossing after L1 accept) and front end busies [23]. The *decorrelated* scalers (one per L1 trigger) count the trigger exposure not correlated with the luminosity profile. These include most of the physics-related AOT and disables such as the individual disables, some global disables, COOR disable, Prescaler (egalitarian algorithm), L2 disable, L3 disable, and Auto-disable. There are no prescales implemented at the other levels of the trigger, so, excluding losses, $\mathcal{L}_{L3} = \mathcal{L}_{L2} = \mathcal{L}_{L1}$.

Unfortunately events can be lost at every stage of the read-out process [21]. It is difficult to correct the luminosity on a trigger-by-trigger basis for these losses given the large rejection factors in the trigger. The solution is to have low-bias triggers that are not rejected by the trigger. These L1 triggers can be used to track losses and correct the luminosity. The *zero bias* trigger fires based on a tick pattern; there is no reliance on detector information. The *min bias* trigger is defined in the same manner as the *zero bias* trigger with the additional requirement of a FastZ signal. Every exposure group normalized by the methods described in these notes must have both a *zero bias* and *min bias* trigger.

The final measure of recorded luminosity is taken from the event catalogs sent to the $\mathcal{L}$DAQ by the datalogging process. These event catalogs contain, for every event in the partition, the event number, LBN, and L1, L2, and L3 trigger masks. Using other information made available to the $\mathcal{L}$DAQ, the *zero bias* and *min bias* triggers can be identified and summed for each luminosity block. This count of recorded triggers is compared to the count

of L1 accepts and used to correct the luminosity for every trigger as follows,

$$\mathcal{L}_{recorded}(n) = \frac{\#zero\ bias_{recorded} + \#min\ bias_{recorded}}{\#zero\ bias_{L1} + \#min\ bias_{L1}}\ \mathcal{L}_{L1}(n). \quad (3)$$

It must be noted that this correction methodology requires that the *zero bias* and *min bias* triggers are handled in exactly the same manner as the other triggers — differences bias the recorded luminosity. Any losses not accounted for by this method must be included in the trigger efficiency.

6 Status of DØ

The Tevatron delivered $\approx 68\ pb^{-1}$ of luminosity from October 8, 2000 through August 23, 2002. This luminosity, integrated over time, is display in Fig. 10. The delivered luminosity is defined using Eq. 1. Luminosity delivered during operations, that is, luminosity delivered while a recorded run was going (discounting all sources of disable during a run including COOR disables associated with pauses) is labeled as utilized in Fig. 10. Down-time is shown in Fig. 11 (left) as a function of date. The points are the average down-time on a calendar day during a store, the histogram is the seven-day average. The down-time is $\approx 15\%$ with large fluctuations.

There are two methods for extracting the live fraction. One method uses the correlated and decorrelated scalers associated with zero-bias triggers to measure the fraction of exposed ticks. This is the quantity shown in Fig. 11 (right) and in Fig. 12 (left). The latter figure also shows the dead fraction associated with correlated and decorrelated sources of disable. The second method is based on counts of zero-bias triggers. The live fraction is defined to be the number of zero-bias triggers at L1 divided by the total number expected,

$$Live\ Fraction = \frac{\#zero\ bias\ triggers}{\#crossings/prescale}. \quad (4)$$

This quantity includes all L1 disables by construction. A comparison between the two methods is displayed in Fig. 12 (right).

The live luminosity (Fig. 10) is slightly more ambiguous. It is defined as the largest L1 luminosity for each luminosity block summed over the time period displayed. Typically, this is equal to the live fraction $\times$ the delivered luminosity. In some cases, however, there are differences as some triggers may have abnormally large exposure, for example, triggers associated with test runs. Two curves are included in Fig. 10, one for all runs, and the other limited to triggers belonging to identified physics runs. Both quantities will become more ambiguous as DØ adopts multiple exposure groups within the global physics run.

Major improvements to the data acquisition system between the readout crates and the L3 trigger system were made during the period covered by this report [15]. These improvements are best exemplified by Fig. 13 (left) which shows the efficiency for passing events through the DAQ. There were major losses of luminosity associated with the DAQ prior to the February upgrade. These losses averaged ≈ 20 to 30% and wildly fluctuated from luminosity block to luminosity block. Following the upgrades, these losses dropped to $< 5\%$ and are primarily associated with readout crate problems. These improvements are also

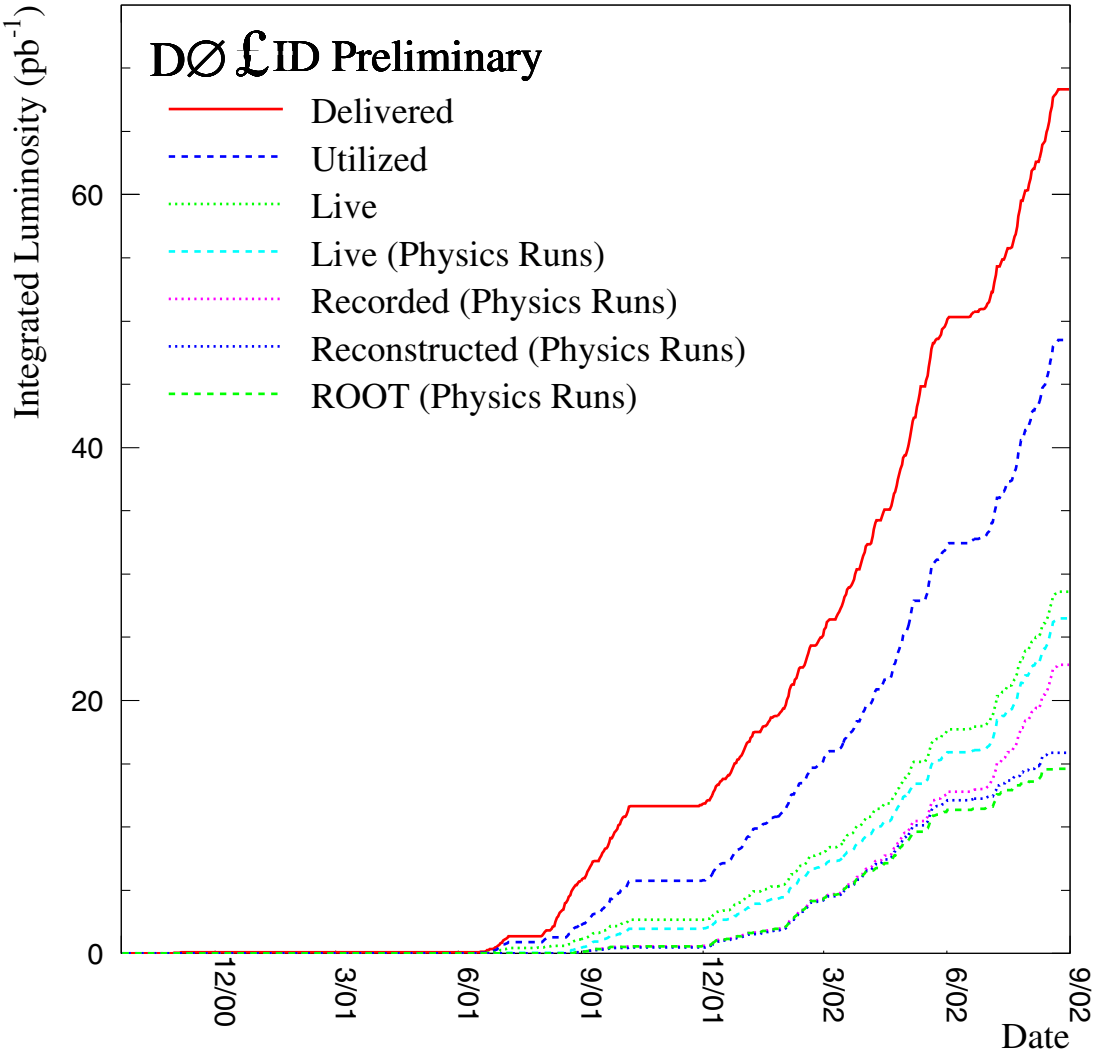

Figure 10: Accumulated luminosity as a function of time.

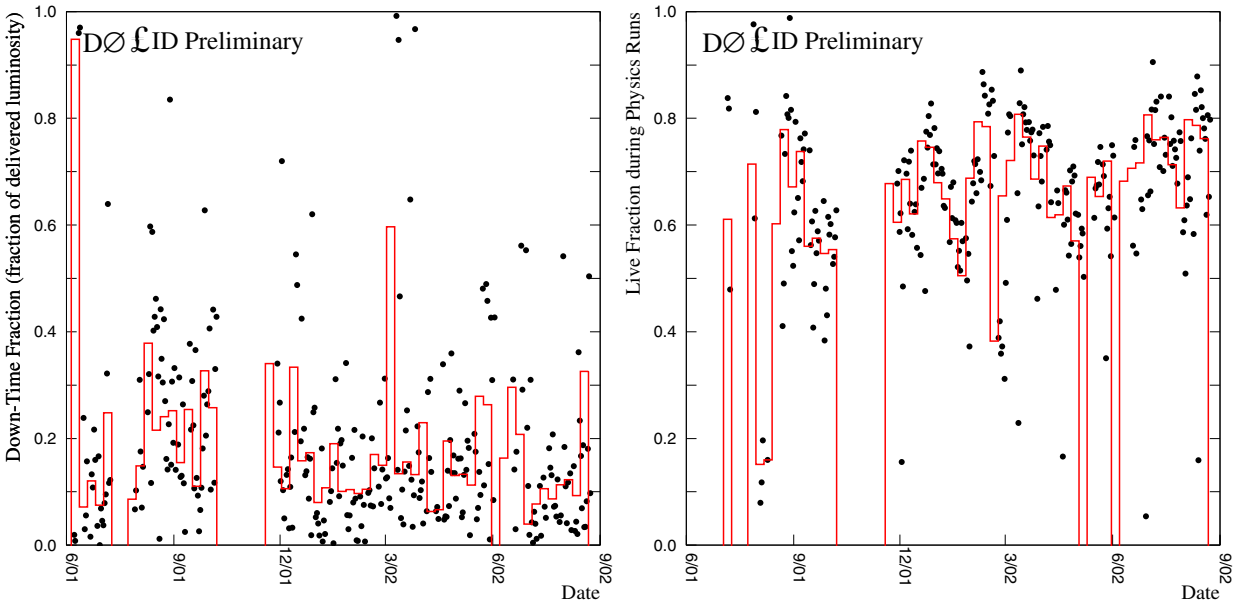

Figure 11: Left: Down-time as a function of date. Right: Live fraction during physics runs as a function of date. Each point is the average over a single day; the histogram is the average over 7 days.

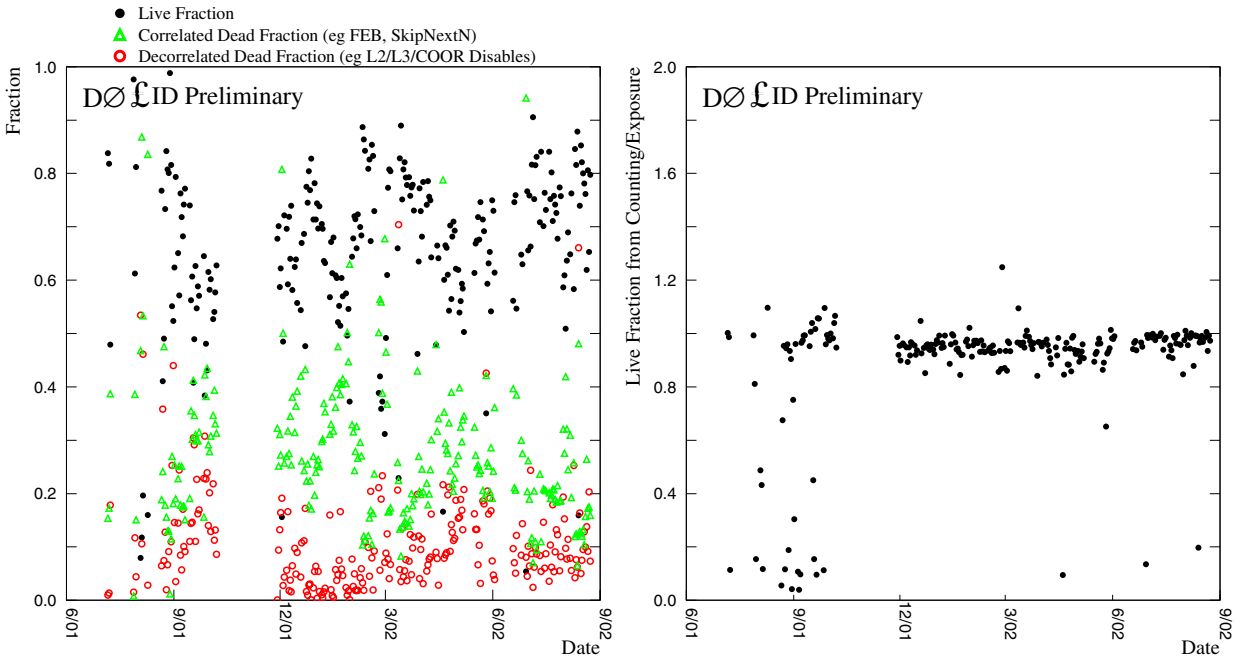

Figure 12: Left: Live fraction (closed circles), correlated dead fraction (triangles), and decorrelated dead fraction (open circles) as a function of date. Right: Comparison between the two methods of calculating live fraction.

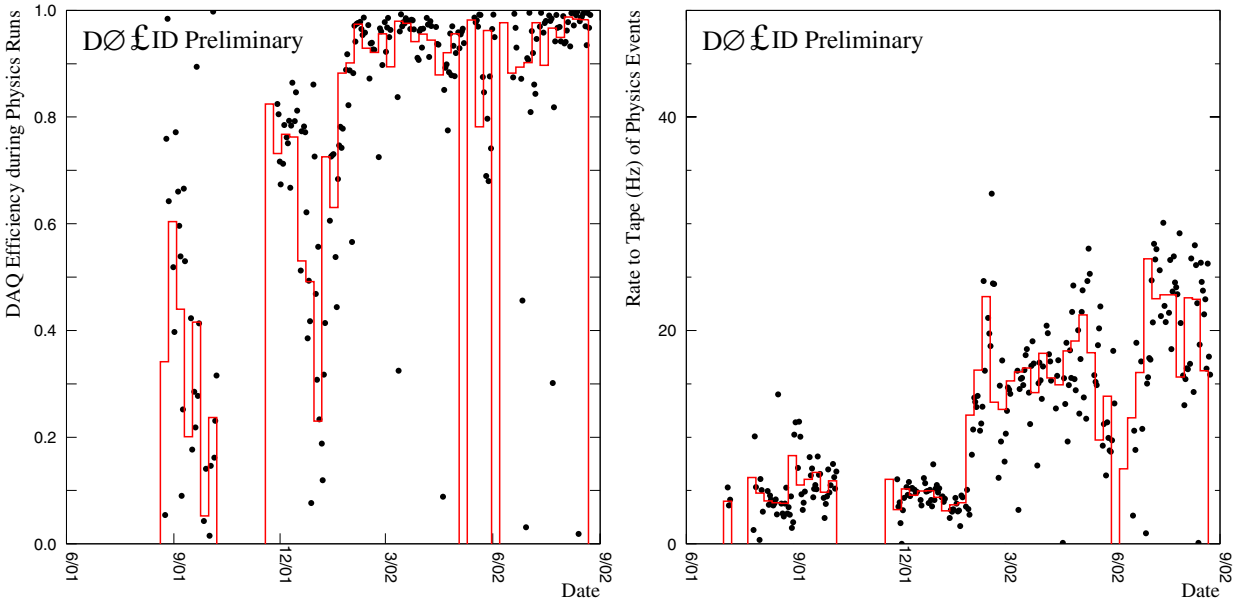

Figure 13: Left: Efficiency for passing events through the data acquisition system between the read-out crates and L3. Right: Rate at which events were stored to disk by the Datalogger process as a function of date. Each point is the average over a single day; the histogram is the average over 7 days.

evident in Fig. 13 (right) which shows the rate-to-tape for physics runs. This improvement has enabled the experiment to keep up with increases in delivered luminosity (Fig. 14) and the number of events (Fig. 15 (right)).

Large losses of luminosity after L1 continue to be a problem for DØ. Additional losses, over and above any losses in the data acquisition [15], L3, or Online systems [7], originate in the offline data processing. The culmination of the Online system is the placement of raw data files on tape [7]. Data files are read back off these tapes by the offline farms for processing using certified versions of the reconstruction software. By construction, files containing events that cause crashes in the reconstruction software may not be included in normalized analysis. Other files are lost due to unreadable tapes, mistakes in the runs configuration or data processing (SAM) [25] databases, and improper handling.

The Luminosity ID group has analyzed the contents of these databases; the results are displayed in Figs. 15. Of the ≈ 114 million events we've accumulated to date, ≈ 79 million have been successfully processed by the reconstruction software. We've also processed most of the Root-tuples produced by the analysis software [26]. This processing includes counts of every trigger in the Root-tuples. These counts are compared to the number of recorded events. Any differences between these values cause the Luminosity Block to be considered bad for that trigger.

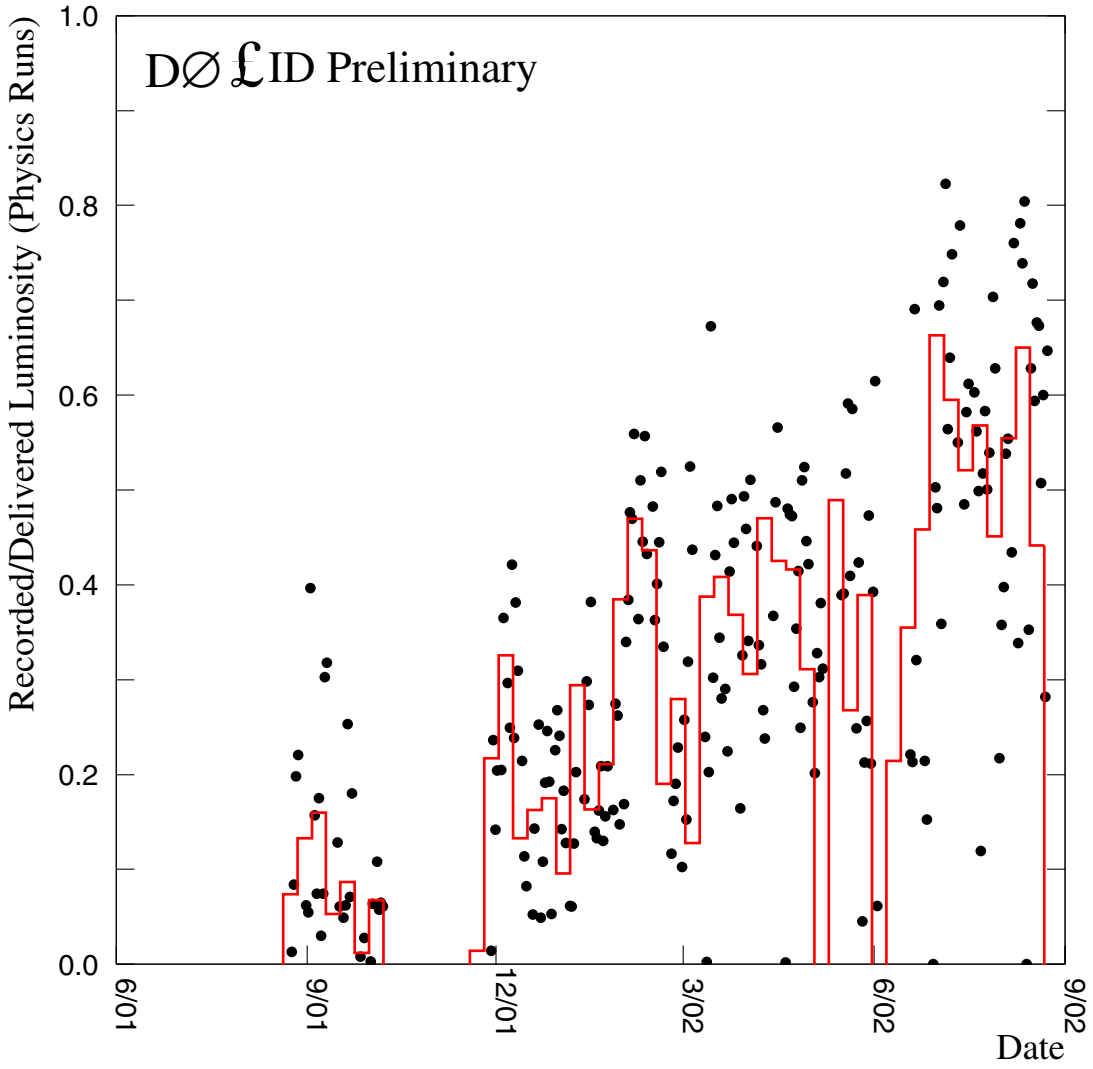

Figure 14: Ratio of recorded to delivered luminosity. Each point is the average over a single day; the histogram is the average over 7 days.

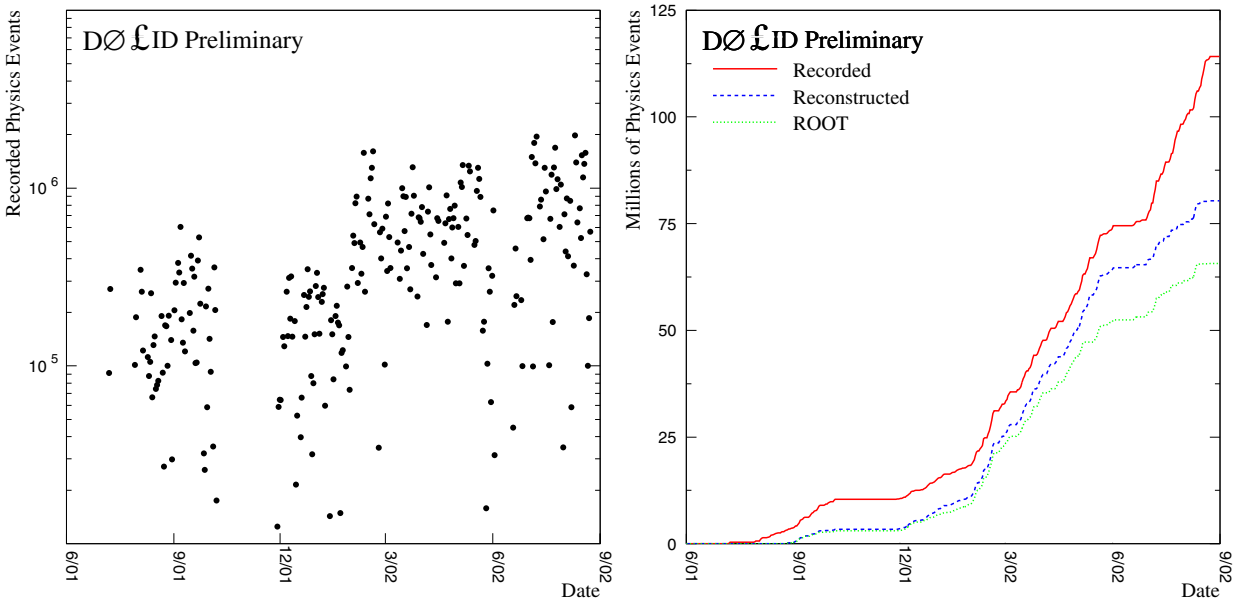

Figure 15: Left: Number of recorded physics events by day. Right: Number of physics events recorded, reconstructed, and converted into Root-tuples integrated over time.

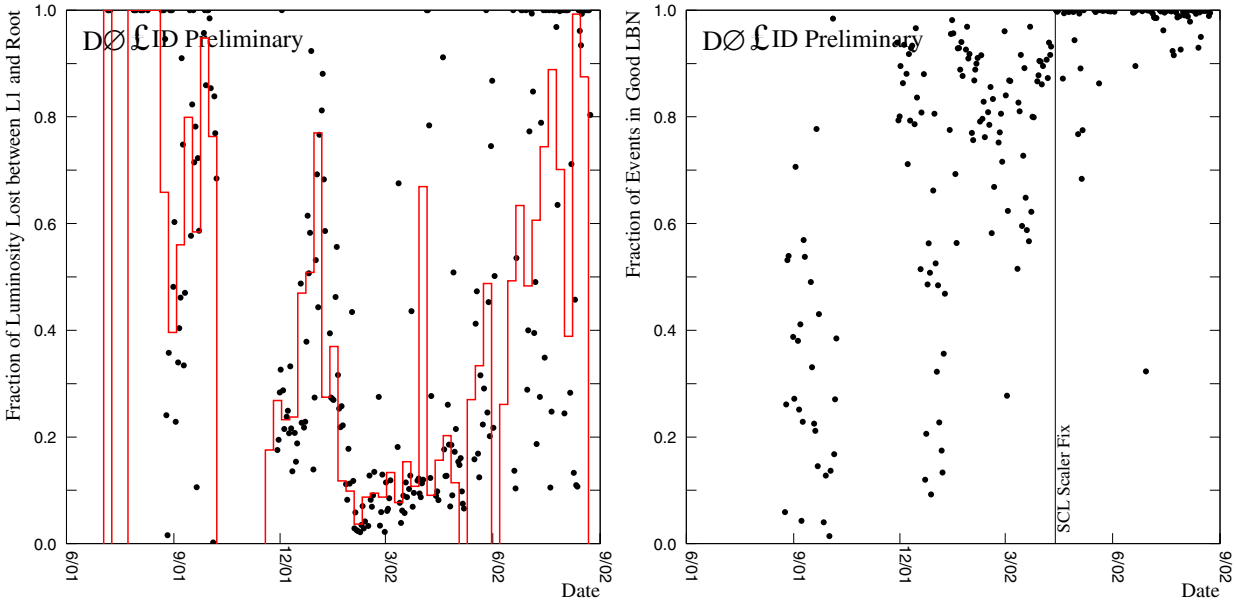

Figure 16: Left: Fraction of luminosity lost between the L1 accept and the Root-tuple file. Each point is the average over a single day; the histogram is the average over 7 days. Right: Fraction of events in good luminosity blocks by day.

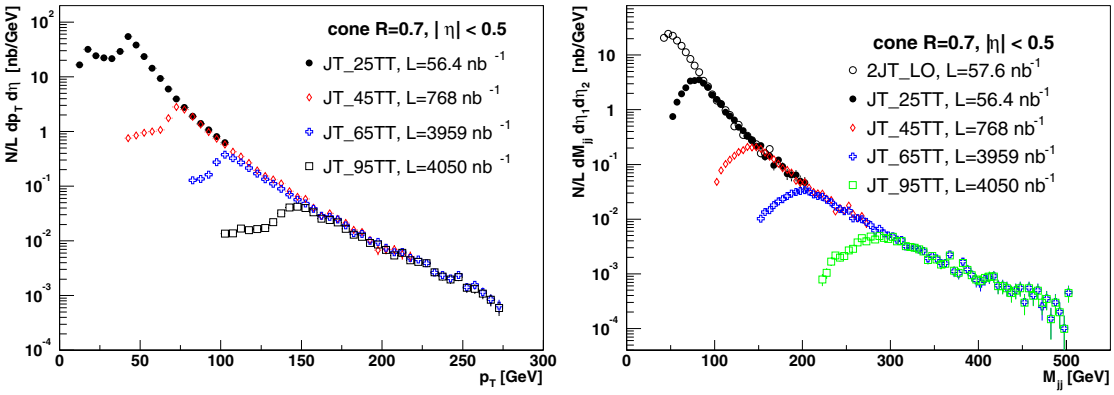

Figure 17: Left: Jet inclusive p_T spectrum in the central calorimeter region ($|\eta| < 0.5$) for a cone with $R = 0.7$. Right: Di-jet mass spectrum.

7 Normalization

The Luminosity ID group has created a package called `lm_access` [18] that provides interfaces for normalizing data. This package is available from the DØ CVS repository. `lm_access` includes classes and methods to provide L1, recorded, and reconstructed luminosities, integrated over a luminosity block, with appropriate status information. *It is essential that events in* **bad** *luminosity blocks be* **removed** *from any normalized analysis. There is no way to correct for losses in bad luminosity blocks.* Most of these losses (Fig. 16 (right)) are due to bad scaler information, typically associated with non-luminosity related hardware failures that require a reinitialization of the serial command link.

Each LBN has an ASCII file with the necessary information for calculating the integrated luminosity by trigger. Luminosity files are cached on `d0mino` and `clued0` and are regularly updated. A simple example showing how to calculate the luminosity and cross section for one particular trigger can be found in the `lm_access` documentation. Luminosity information are accessed via the class `LumFileMap`. A list of LBNs associated with the data are kept in memory organised according to the version of the reconstruction software. The user specifies the list of triggers to normalize and the type of luminosity (triggered, recorded, or reconstructed). The reconstructed luminosity is sensitive to the version of the reconstruction software. A method returns the integrated luminosity in μb^{-1} for each requested trigger. The results from a jet analysis (single and di-jet normalized number distributions) are shown in Fig. 17. The jet triggers in this analysis have varying prescales; the normalization information is used to correct for these and other effects.

7.1 Normalizing Stripped Datasets

It is important to preserve the list of LBNs in the parent data sample to properly compute the luminosity of a stripped dataset. In particular, it is essential to include luminosity blocks for which a given trigger was exposured, but during which the trigger never fired (e.g., a rare Higgs trigger). The officially produced non-stripped files have already been properly

accounted for in the normalization process (the reconstructed luminosity referred to above).

The situation is more complicated in the case of stripped data files because different groups have stripped the data in different ways. The approach described above cannot be used usually since there is no guaranty that there is at least one event per LBN in the stripped data files. It is up to the individual group to keep the list of original LBNs corresponding to their parent sample and to provide tools that incorporate this list in the data analysis.

8 Conclusions

The Luminosity Monitor (with the Run 1 electronics) and the luminosity data acquisition system operated relatively smoothly over the period covered in this note. There was very little down-time associated with these two systems. We recorded $\approx 68\ pb^{-1}$ delivered to DØ by the Tevatron between October 8, 2000 and August 23, 2002. As a whole, the DØ experiment has greatly improved in data rate and efficiency over the past year. We placed $\approx 23\ pb^{-1}$ associated with global physics runs on tape and processed close to $\approx 15\ pb^{-1}$. These data have been used in several normalized physics analyses including the measurement of the W and Z cross sections [27].

References

[1] J. Bantly *et al.*, *The Level 0 Trigger for the DØ Detector*, DØ Note 1996.

[2] M. A. Tartaglia and D. P. Owen, *A Comparison of FastZ and SlowZ Luminosity Monitors*, DØ Note 2879.

[3] C.-C. Miao, *The DØ Run II Luminosity Monitor*, Nucl. Phys. Proc. Suppl. **78**, 342 (1999), DØ Note 3573.

[4] C.-C. Miao and R. Partridge, *Study of the Run II Luminosity Monitor Counter Design*, DØ Note 3319.

[5] D. Edmunds *et al.*, *Level 1 Trigger OR's with Pseudo-AND/OR Terms*, DØ Note 3683.

[6] S. H. Ahn *et al.*, *Design of the Data Acquisition System for Measuring DØ Luminosity*, DØ Note XXXX.

[7] S. Fuess *et al.*, *The DZERO Online System Event Path*, DØ Note 3982.

[8] D. Genser, *Intertask Communication (ITC) Package*, 2000.

[9] D. C. Schmidt, "The ADAPTIVE Communication Environment: Object-Oriented Network Programming Components for Developing Client/Server Applications," 11^{th} and 12^{th} Sun Users Group Conference, San Jose, California, December 1993 and June 1994.

[10] G. van Rossum *et al.*, *Python Reference Manual*, PythonLabs, 2001.

[11] S. H. Ahn *et al.*, *Real-Time Monitoring of the Luminosity System*, DØ Note 3967.

[12] M. Abolins *et al.*, *DØ Run II Level 1 Trigger Framework Technical Design Report*, 1998.

[13] S. H. Ahn *et al.*, *Communications between DØ and the Beams Division*, DØ Note XXXX.

[14] J. F. Bartlett *et al.*, *The Control Architecture of the DØ Experiment*, DØ Note 3931.

[15] B. Angstadt *et al.*, "Ethernet-based Data Acquisition for the DØ Experiment at Fermilab," contributed to the 6th World Multiconference on Systemics, Cybernetics and Informatics (SCI 2002), Orlando, Florida, July 14—18, 2002.

[16] A. Boehnlein *et al.*, *Interactions between the Level 3 framework and ScriptRunner*, DØ Note 3631.

[17] S. Snyder, *COOR*, 2002.

[18] S. H. Ahn *et al.*, *Accessing Triggered Luminosity Information via Flat Files*, DØ Note 3969.

[19] S. H. Ahn *et al.*, *DØ Luminosity in Run 2: Delivered*, DØ Note 3970.

[20] S. H. Ahn *et al.*, *DØ Luminosity in Run 2: Triggered*, DØ Note 3971.

[21] S. H. Ahn *et al.*, *DØ Luminosity in Run 2: Recorded*, DØ Note 3972.

[22] J. Bantly *et al.*, *DØ Luminosity Monitor Constant for the 1994—1996 Tevatron Run*, DØ Note 3199.

[23] D. Edmunds *et al.*, *Online measurement of Beam Luminosity and Exposed Luminosity for Run II*, 1997.

[24] H. Schellman *et al.*, *Summary of the Luminosity Workshop — September 17-18, 1998*, DØ Note 3523.

[25] J. Bakken *et al.*, *Requirements for the Sequential Access Model Data Access System*, DØ Note 3465.

[26] S. H. Ahn *et al.*, *User Interface to Find the Luminosity Blocks Corresponding to Data Files*, DØ Note 3937.

[27] M. Kado and R. Zitoun, *Measurement of the Z and W boson production cross sections in the electron mode in $p\bar{p}$ collisions at 1.96 TeV*, DØ Note 4003.